Nucleic Acids Research, 1993, Vol. 21, No. 8 ***1919–1925***

Ribonuclease III cleavage of a bacteriophage T7 processing signal. Divalent cation specificity, and specific anion effects

Hong-Lin Li, Bhadrani S.Chelladurai, Kejing Zhang and Allen W.Nicholson*
Department of Biological Sciences, Wayne State University, Detroit, MI 48202, USA

Received December 12, 1992; Revised and Accepted March 3, 1993

ABSTRACT

***Escherichia coli* ribonuclease III, purified to homogeneity from an overexpressing bacterial strain, exhibits a high catalytic efficiency and thermostable processing activity *in vitro*. The RNase III-catalyzed cleavage of a 47 nucleotide substrate (R1.1 RNA), based on the bacteriophage T7 R1.1 processing signal, follows substrate saturation kinetics, with a K_m of 0.26 μM, and k_{cat} of 7.7 min.$^{-1}$ (37°C, in buffer containing 250 mM potassium glutamate and10 mM $MgCl_2$). Mn^{2+} and Co^{2+} can support the enzymatic cleavage of the R1.1 RNA canonical site, and both metal ions exhibit concentration dependences similar to that of Mg^{2+}. Mn^{2+} and Co^{2+} in addition promote enzymatic cleavage of a secondary site in R1.1 RNA, which is proposed to result from the altered hydrolytic activity of the metalloenzyme (RNase III 'star' activity), exhibiting a broadened cleavage specificity. Neither Ca^{2+} nor Zn^{2+} support RNase III processing, and Zn^{2+} moreover inhibits the Mg^{2+}-dependent enzymatic reaction without blocking substrate binding. RNase III does not require monovalent salt for processing activity; however, the *in vitro* reactivity pattern is influenced by the monovalent salt concentration, as well as type of anion. First, R1.1 RNA secondary site cleavage increases as the salt concentration is lowered, perhaps reflecting enhanced enzyme binding to substrate. Second, the substitution of glutamate anion for chloride anion extends the salt concentration range within which efficient processing occurs. Third, fluoride anion inhibits RNase III-catalyzed cleavage, by a mechanism which does not involve inhibition of substrate binding.**

INTRODUCTION

Bacterial RNA processing is carried out by a functionally diverse collection of specific ribonucleases [1–4]. A prominent component of the *Escherichia coli* RNA processing machinery is ribonuclease III (RNase III; E.C.3.1.24). RNase III catalyzes the cleavage of phosphodiester bonds within its processing signals, which are found within cellular, viral and plasmid transcripts, and which feature dsRNA as a common structural motif (see [5–7] for reviews). RNase III can control mRNA translational efficiencies, and RNA physical and functional half-lives. Current evidence indicates that RNase III-catalyzed cleavage can remove RNA sequences which would otherwise impede productive binding of mRNA to the 30S ribosomal subunit, or block the action of degradative ribonucleases [8–10]. RNase III may also control translation initiation by acting as an mRNA-binding protein [11]. However, the molecular mechanisms which link RNase III processing to mRNA translational efficiencies or turnover rates have yet to be definitively described.

RNase III processing activity is exhibited by a 52 KDa homodimeric species, which catalyzes out divalent metal ion-dependent hydrolytic cleavage of substrate, creating RNA products with 5′-phosphate and 3′-hydroxyl termini. We have previously shown that the 2′-hydroxyl group adjacent to the scissile bond is not essential for catalysis [12], and that RNase III is tolerant towards modified phosphodiester linkages [13]. However, the kinetic pathway for RNase III processing is not known. Mechanistic studies are now possible, with the availability of small, specific processing substrates [14] and purified RNase III [15,16; this report]. We describe below an initial enzymological study of RNase III, purified to near-homogeneity by an efficient method that is a modification of two previously-described procedures. We present the steady-state enzymatic parameters (K_m, k_{cat}) for the RNase III-catalyzed cleavage *in vitro* of a small substrate, based on the bacteriophage T7 R1.1 processing signal. The *in vitro* catalytic efficiency of RNase III is compared to its *in vivo* processing activity. The dependence of RNase III processing on divalent metal ion type and concentration, and on monovalent salt concentration and anion type is described.

MATERIALS AND METHODS

Materials

Chemicals and reagents were of the highest quality commercially available. Water was purified using a Millipore Milli-Q Plus system. Ribo- and deoxyribonucleoside triphosphates, and AG Poly(I)-poly(C) agarose were from Pharmacia-LKB (Piscataway,

* To whom correspondence should be addressed

NJ). Dupont-NEN (Boston, MA) was the source of [α-^{32}P]UTP (3000 Ci/mmol) and [α-^{35}S]dATP (1000 Ci/mmol). [^{3}H]-poly r(A-U) (specific activity, 3.5×10^{5} dpm/pmol polymer phosphorus) was synthesized as described [17] using poly d(A-T) (Pharmacia-LKB), [5,6-^{3}H]UTP (ICN, Irvine, CA; 37.5 Ci/mmol), ATP and *E.coli* RNA polymerase (Promega, Inc., Madison, WI). The BCA* protein assay kit was from Pierce (Rockford, IL). DNase I was from Promega, while restriction enzymes, Tli ('Vent') DNA polymerase, and T4 DNA ligase were from New England Biolabs (Beverly, MA). Sequenase (v.2) was from United States Biochemical Corp. (Cleveland, OH), and dideoxy DNA sequencing was carried out according to the supplier's instructions. T7 RNA polymerase was purified as described [18], using *E.coli* BL21 containing plasmid pAR1219 (provided by J. Dunn). Plasmid pET-11a was from Novagen (Madison, WI), and plasmid pAR2916, encoding the RNase III (*rnc*) structural gene, was provided by A. Rosenberg. DNA oligonucleotides were synthesized from 3′-β-cyanoethylphosphoramidite, 2′-deoxyribonucleoside precursors, and purified as described [14]. The synthesis of the ^{32}P-labeled R1.1 RNA processing substrates is described in the legend to Figure 2.

Methods

Cloning the rnc gene in a T7 expression vector. The *rnc* gene in pAR2916 was isolated by PCR amplification, using as *rnc* 5′ primer, 5′-GGG**CATATG**AACCCCATCGTA-3′ and as *rnc* 3′ primer, 5′-CCC**GGATCC**TCATTCCAGCTC-3′. The 5′ primer carried an *Nde*I site (indicated in bold face), and the *rnc* AUG initiation codon (underlined), while the 3′ primer encoded a *Bam*H1 site (bold face) directly adjacent to the sequence complementary to the *rnc* stop codon (underlined). The reaction (100 μl) contained in the specified buffer: 4 fmol plasmid DNA, 30 pmol each of the 5′ and 3′ primers, 200 μM of each dNTP, 1 mg BSA, and 2.5 units Vent DNA polymerase. The PCR cycle (repeated 30 times) was: 94°C (1 min.), 40°C (1 min.), 55°C (1 min.), and 72°C (3 min.). The agarose gel-purified product (696 bp) was digested with *Nde*1 and *Bam*H1, repurified by gel electrophoresis, and ligated (at 5−6°C for 48 hr, using 1 unit of T4 DNA polymerase in a 20 μl reaction) to gel-purified, *Nde*1/*Bam*H1-digested pET-11a DNA. HMS174 cells were transformed with an aliquot of the ligation reaction. Recombinant plasmids were identified by restriction analysis, and a plasmid isolate (pET-*rnc*) was introduced into HMS174(DE3) cells. The *rnc* gene in pET-*rnc* was sequenced by the dideoxy method, using the *rnc* 5′ and 3′ PCR primers (see above), Sequenase, and [α-^{35}S] dATP. Sequences adjacent to the primers were obtained by the Mn^{2+} substitution method. The cloned *rnc* sequence agreed completely with the published sequence [19].

Purification of RNase III. RNase III was isolated by a method based on two previously described protocols [15,20]. HMS174(DE3)/pET-*rnc* cells were grown at 37°C in 500 ml LB medium (40 μg/ml Ampicillin) with vigorous shaking to an OD_{600} of 0.5. IPTG (0.2 mM) was then added, and incubation continued at 37°C for 3−4 hours. There occurred the rapid production of a 26 KDa polypeptide, which accumulated to about 50% of total cellular protein, 4 hours post-induction (Figure 1). The following steps were carried out at 4−6°C. Cells (approximately 4 g wet weight) were collected by centrifugation, washed with 15 ml of 50 mM Tris−HCl (pH 8.0), 25% sucrose, then treated for 15 minutes with 15 ml of the same buffer containing 0.5 mg/ml egg white lysozyme. Lysis buffer [1% Nonidet P-40, 0.5% sodium deoxycholate, 0.1 M NaCl, 30 mM Tris−HCl (pH 8.0), 1 mM DTT, 1 mM EDTA; 20 μg/ml PMSF] was added, followed by $MgCl_2$ (5 mM) and DNase I (10 units/ml), then incubated for 10 minutes. The overexpressed *rnc* polypeptide was initially obtained as an inclusion body. Following centrifugation (10,000×g, 15 minutes), the pellet was washed four times with lysis buffer, then twice with 50 mM Tris−HCl (pH 8.0), 5 mM $MgCl_2$ and 1 mM DTT. The washed pellet was treated for 30 minutes with 20 ml of 8% ammonium sulfate, 25 mM Tris−HCl (pH 8.0), 20 mM 2-mercaptoethanol, and 0.1 mM EDTA. Following a brief centrifugation, the clarified supernatant was loaded onto a 3 cm column of AG poly(I)-poly(C) agarose (2 ml bed volume; flow rate, 0.3 ml/minute), which was then washed with 4 volumes of 1 M NH_4Cl. RNase III was eluted with 2M NH_4Cl, dialyzed against storage buffer (50% glycerol, 0.5 M KCl, 30 mM Tris−HCl (pH 8.0), 0.1 mM EDTA, 0.1 mM DTT), then applied to a SuperDex 75 gel filtration column (Pharmacia-LKB) (flow rate, 0.5 ml/minute). The major UV-absorbing peak, corresponding to the dimeric form of RNase III, was well separated from lower molecular weight, UV-absorbing material.

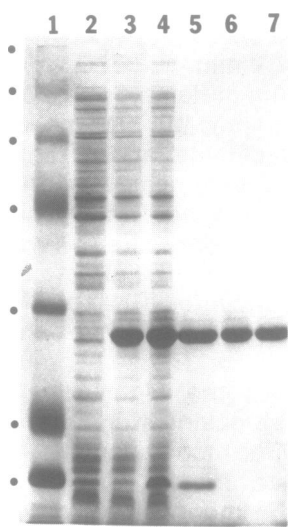

Figure 1. Purification of overexpressed RNase III. Production of the 26 KDa *rnc* polypeptide was accompanied by greatly enhanced levels of RNase III processing activity in cell extracts. The 26 KDa species was not observed in IPTG-treated cells carrying the parent pET-11a vector (data not shown). Aliquots of cell lysates, or of protein fractions obtained during purification were analyzed by electrophoresis in a 12% polyacrylamide gel containing 0.1% SDS in Tris-glycine buffer [39]. Gels were stained with Coomassie Brilliant Blue R, then destained, dried and photographed. The relative amount of stained *rnc* polypeptide was estimated by optical imaging using an Ambis unit. Lane 2 displays proteins in an aliquot (15 μl) from a lysate (100 μl) derived from a 1 ml LB (+ Ampicillin) culture of HMS174(DE3) cells carrying pET-*rnc* (no IPTG addition) grown to saturation. Lane 3, same as lane 2, except 4 hours following IPTG addition. Lanes 4−7, analysis of protein during purification. Lane 4, protein in initial lysate (15 μg); lane 5, 8% ammonium sulfate fraction (4 μg); lane 6, fraction eluting from Poly(I)-poly(C) agarose (3 μg); lane 7, SuperDex 75 gel filtration sample (3 μg from fraction 11). Two minor species (<2% of total protein) were occasionally observed in the purified protein preparations (see lanes 5 and 6). These proteins migrated slightly more slowly than the *rnc* polypeptide, and may be *rnc*-related. Lane 1 displays prestained protein size markers (GIBCO-BRL, Grand Island, NY). From top to bottom, the M_r values are: 200, 97.4, 68, 43, 29, 18.4 and 14.3 KDa.

The protein concentration in the peak fractions ranged from 0.1−0.5 mg/ml, and the fractions were directly stored at −20°C. When required, enzyme was concentrated about 10-fold using a Centriprep unit (Amicon; 10,000 MW cut-off). The procedure routinely provided 6−7 milligrams of enzyme (≥95% purity), from 4 g of cells. The rapidity of the procedure (approximately 10 hours from cell lysis), and the inclusion of a reducing agent and protease inhibitor helped ensure the physical integrity and activity of RNase III. Also, care was taken to avoid low salt (<250 mM M^+) buffers, which promoted formation of insoluble RNase III aggregates (H.L. and A.W.N., unpublished observations).

Amino acid analysis of purified RNase III (data not shown) was in excellent agreement with the predicted *rnc* amino acid sequence [20]. The BCA* protein assay (using BSA as a standard) overestimated the amount of RNase III by two-fold. Therefore, a correction factor (0.52) was applied, as provided by the amino acid analysis. The measured molar extinction coefficient (280 nm) was 6.5×10^4 M^{-1} cm^{-1} ($A^{1\%}$= 12.5), which is in accord with the predicted content of tryptophan, tyrosine and phenylalanine in the *rnc* polypeptide [20]. The specific activity of purified RNase III was determined by measuring the cleavage rate of ^{3}H-poly r(A-U), using the standard TCA precipitation assay [19]. The specific activity of purified RNase III was 1.9×10^5 units/mg (dimer), which is comparable to the activitiy of enzyme in the 8% ammonium sulfate and poly(I)-poly(C) fractions. The measured specific activity is about 20-fold higher than the values reported in the original purification procedure [6,20]. Two recently-described RNase III purification protocols [15,16] did not report specific activities.

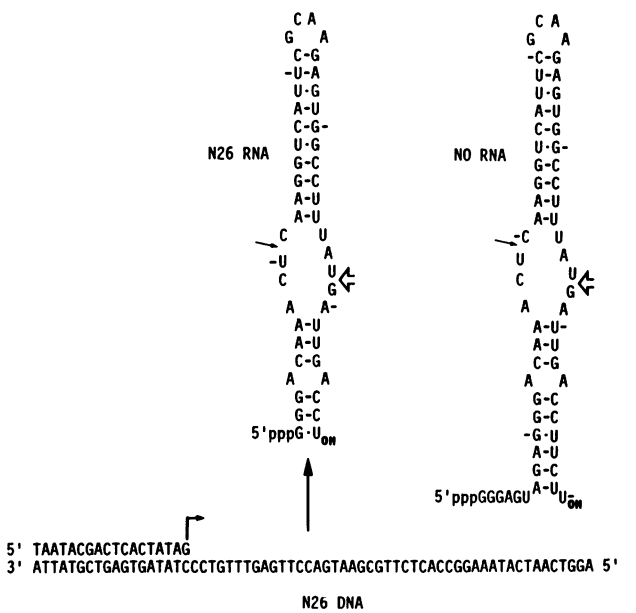

Figure 2. Primary and secondary structures of the T7 phage R1.1 processing signal-based substrates, N0 RNA and N26 RNA. Also shown is the N26 RNA template (64 nt), annealed to its promoter oligonucleotide (18 nt). The bent arrow indicates the transcription startsite. The N0 template is described elsewhere [14]. The primary and secondary RNase III cleavage sites in each RNA are indicated by the large open arrow and small arrow, respectively. Every tenth nucleotide is indicated by a tic mark. The primary cleavage sites in N0 RNA (60 nt) and N26 RNA (47 nt) correspond to the canonical (*in vivo*) site in the T7 R1.1 processing signal [40]. Enzymatic synthesis of the ^{32}P-labeled RNA substrates was performed essentially as described [41]. DNA template (25 pmol) and promoter oligonucleotide (30 pmol) were annealed (70°C, 5 min.; 25°C, 30 min.) in 50 μl of 10 mM Tris−HCl (pH 8.0). A portion of the annealing mix (10 μl) was combined with 1 mM each of the 4 rNTPS, [α-^{32}P UTP] (20 μCi) and 400 units of T7 RNA polymerase in standard buffer [22] (100 μl final volume), and incubated for 4 hours at 37°C. An equal volume of loading buffer (20 mM EDTA, 89 mM Tris, 89 mM boric acid, 20% sucrose and 0.01% each bromphenol blue and xylene cyanol) was added, and samples were electrophoresed in 15% polyacrylamide gels containing 7 M urea in TBE buffer. The RNAs were recovered by phenol extraction of crushed gel bands, followed by ethanol precipitation. Purified RNAs were stored in water at −20°C. The N26 RNA cleavage site was mapped by measuring gel electrophoretic mobilities of the RNase III cleavage products, and by reference to the previously determined N0 RNA cleavage site [14].

RNase III processing assays. The standard 'physiological salt' reaction buffer (see also Results) contained: 250 mM potassium glutamate, 10 mM $MgCl_2$, 30 mM Tris−HCl (pH 7.5), 5 mM spermidine, 0.1 mM DTT, 0.1 mM EDTA, and 0.4 mg/ml *E.coli* tRNA. 'Low salt' reaction buffer specifically omitted potassium glutamate. In some experiments, potassium glutamate was replaced by potassium chloride at the indicated concentration. Unless otherwise reported, the RNase III concentration (dimer) was 10 nM. Reaction mixes containing ^{32}P-labeled RNA substrate (prepared as described in the legend to Figure 2) were prepared on ice in Mg^{2+}-free reaction buffer, with RNase III added last (diluted as necessary in the same buffer). Mg^{2+} was added to initiate cleavage, and the samples incubated at the specified temperature. The reactions were terminated by the addition of an equal volume of reaction stop mix (20 mM EDTA, 89 mM Tris, 89 mM Boric acid, 20% sucrose, and 0.01% each of bromphenol blue and xylene cyanol), and aliquots were electrophoresed (25 V/cm) in 15% polyacrylamide gels containing 7 M urea in TBE buffer. Autoradiography was carried out at −70°C using Fuji RX film and intensifying screens. Quantitative determination of RNA precursors and products was performed using an Ambis radioanalytic imaging system (2.8% counting efficiency). Assays were performed in duplicate, and agreed to within 10%.

RESULTS

Purification and properties of RNase III

RNase III processing activity was followed during purification using ^{32}P-labeled R1.1 RNA (N0 RNA; Figure 2) as substrate. Specifically, analysis of the gel filtration column eluent revealed that the fractions containing RNase III processing activity directly overlapped the major UV-absorbing protein peak, and were consistent with an approximately 50 KDa species (data not shown). A lower amount of RNase III processing activity was reproducibly observed in a later fraction, indicating the existence of a species having an M_r value similar to that of the 26 KDa RNase III subunit. The occurrence of RNase III processing activity at this position suggests the (reversible) dissociation of the protein dimer. Alternatively, the monomeric form of the enzyme may possess catalytic activity. This gel filtration behavior of RNase III has been noted elsewhere [22]. RNase III processing activity is thermostable. In separate experiments (data not shown), a two hour preincubation of enzyme at 37°C in reaction buffer caused only a negligable decrease in the initial cleavage rate of ^{32}P-labeled R1.1 RNA (N26 RNA; Figure 2). Moreover, prior heating of purified RNase III at 90°C (in reaction buffer either

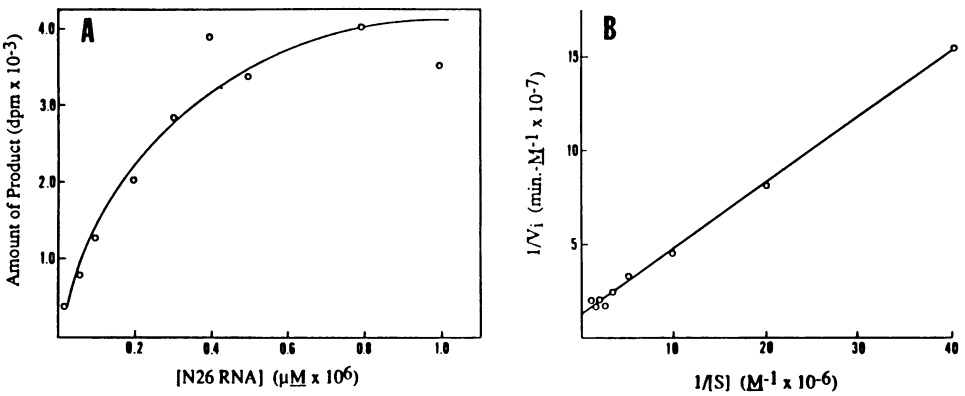

Figure 3. Kinetic analysis of RNase III processing. Panel A displays the concentration dependence of the initial cleavage rate of ^{32}P-labeled N26 RNA (250 mM potassium glutamate reaction buffer,37 °C). Panel B displays the double-reciprocal analysis of the data in Panel A. The steady-state kinetic parameters (K_μ and k_{cat}) are presented in Table I. N26 RNA was the preferred substrate in these experiments, since N0 RNA did not provide reproducible cleavage kinetics at the higher (> 0.5 μM) concentrations. This may have been due to the presence in N0 RNA of a single-stranded, purine-rich sequene at the 5′ end (absent in N26 RNA, see Figure 2), which may promote aggregation at higher concentrations (e.g., see [42]). Alternatively (or in addition) the variability in processing kinetics at higher substrate concentrations may be due to unidentified material which copurifies with the ^{32}P-labeled RNA (B.S.C. and A.W.N., unpublished observations).

with or without Mg^{2+}) for up to one minute did not significantly inhibit enzyme activity. However, all processing activity was lost following a ten minute incubation at 90°C. The high specific activity and thermostability are advantageous properties for the enzymological and physical study of RNase III.

Kinetics of RNase III cleavage of the T7 R1.1 processing signal

To determine the kinetic parameters for RNase III processing in the steady-state, we measured the initial cleavage rate of a specific processing signal as a function of its concentration. The 47 nt substrate (N26 RNA, Figure 2) is based on the bacteriophage T7 R1.1 processing signal [23], and undergoes accurate cleavage at a single site *in vitro* [13,14]. The RNase III concentration (dimer) was 10 nM, the ^{32}P-labeled N26 RNA concentration ranged upwards from 50 nM, and the cleavage rates were measured at 30 and 37°C in reaction buffer containing 250 mM potassium glutamate or potassium chloride (see also below). The dependence of initial cleavage rate on RNA concentration is displayed in Figure 3A; the corresponding double-reciprocal plot is given in Figure 3B, and the parameters are summarized in Table I. RNase III cleavage of the R1.1 processing signal follows substrate saturation kinetics, with a K_m of 0.26 μM, and k_{cat} of 7.7 min.$^{-1}$ at 37°C (Table I). Thus, as anticipated, R1.1 RNA processing involves substrate binding to a saturable site, followed by phosphodiester bond hydrolysis and product release. The K_m value is relatively insensitive to temperature (between 30 and 37°C), while the k_{cat} exhibits a modest increase (Table I). The catalytic efficiency (k_{cat}/K_m) of R1.1 processing (3×10^7 l/mol-min), suggests that the *in vitro* processing activity of RNase III reflects its known *in vivo* catalytic efficiency (see Discussion).

RNase III processing dependence on divalent metal ion

RNase III requires a divalent metal ion, preferably Mg^{2+} for activity [6,21]. Mn^{2+} can also support enzymatic cleavage, with some qualitative differences [21,24,25]. The ability of other divalent metal ions to support processing has not been definitively addressed. We determined the initial cleavage rate of N26 RNA as a function of Mn^{2+}, Co^{2+}, Ca^{2+} or Zn^{2+} concentration, and compared it to the rate of the Mg^{2+}-supported reaction. The results are summarized in Figure 4A, and Figure 4B displays the autoradiogram of the Mn^{2+} experiment. We find that Mn^{2+} and Co^{2+} support accurate enzymatic cleavage of N26 RNA. In contrast, neither Ca^{2+} nor Zn^{2+} support any detectable enzymatic reaction over the concentration range tested [a small amount of enzyme-independent degradation of substrate was observed in the Zn^{2+} experiment (data not shown)]. In 250 mM potassium glutamate reaction buffer, Co^{2+} provides a half-maximal initial cleavage rate at 6 mM, while Mg^{2+} and Mn^{2+} each provide half-maximal rates at 3 mM. Mn^{2+} distinguishes itself in that it supports processing at a relatively low concentration (0.5 mM), which is suppressed between 0.5 and 5 mM (Figure 4B). In addition, Mn^{2+} promotes enzymatic cleavage of the R1.1 RNA secondary site (between U_{10} and C_{11} in N26 RNA) as shown in Figure 5 (lane 19). Co^{2+} also supports secondary site cleavage in a manner similar to Mn^{2+} (data not shown). The transition metal ion-induced alteration in processing behavior is attributed to RNase III 'star' activity (see Discussion).

Since neither Ca^{2+} nor Zn^{2+} support RNase III processing of R1.1 RNA, it was of interest to determine whether these species could inhibit the Mg^{2+}-supported enzymatic cleavage reaction. The initial cleavage rate of R1.1 RNA (in reaction buffer containing 250 mM potassium chloride and 5 mM $MgCl_2$) was measured as a function of added Ca^{2+} or Zn^{2+}. The results, presented in Figure 4C, show that Zn^{2+}, but not Ca^{2+}, inhibits the Mg^{2+}-supported enzymatic cleavage. Half-maximal inhibition of processing occurs at approximately 0.5 mM Zn^{2+}. However, Zn^{2+} does not inhibit formation of the enzyme-

Table I. Kinetic parameters for RNase III cleavage of the T7 R1.1 Processing Signal[a]

Salt[b]	T (°C)	k_{cat} (min^{-1})[c]	K_m (μM)[c]	k_{cat}/K_m (l/mol-min)
KGlu	37	7.7	0.26	3.0×10^7
KGlu	30	7.2	0.26	2.8×10^7
KCl	30	5.6	0.23	2.4×10^7

[a] K_m and k_{cat} values were determined by measuring the initial rate of production of the 38 nt (5′ end-containing) cleavage product of N26 RNA, as a function of substrate concentration (see Materials and Methods). Linear regression analysis was carried out on the data provided by the double reciprocal plot (Figure 4B).
[b] 250 mM salt concentration in all cases; KGlu, potassium glutamate.
[c] Maximum error limits are ±0.5 min.$^{-1}$ for the k_{cat} values, and ± 0.03 μM for the K_m values.

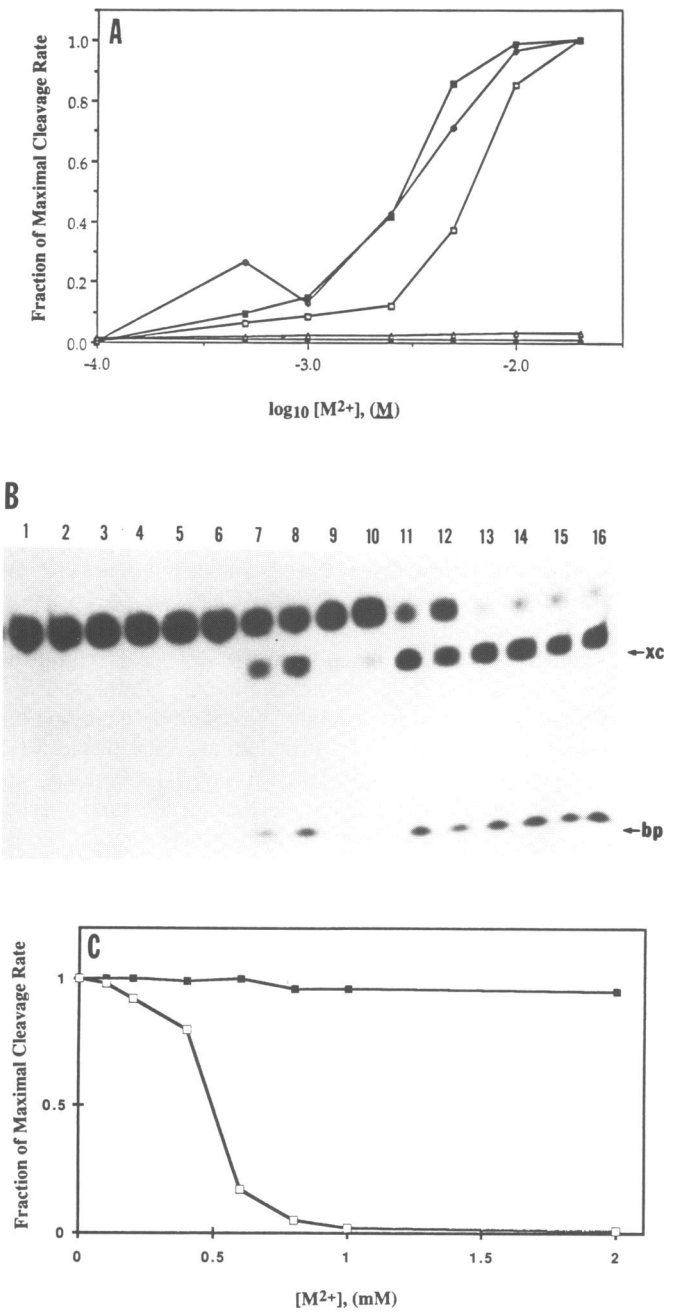

Figure 4. Divalent cation dependence of RNase III processing. Initial cleavage rates of ^{32}P-labeled N26 RNA were measured in 250 mM potassium glutamate reaction buffer at 37°C, as described in Materials and Methods. (**A**) Percent maximal cleavage rate versus concentration (mM) of $MgCl_2$ (■), $MnCl_2$ (◇), $CoCl_2$ (□), $CaCl_2$ (△), and $ZnCl_2$ (●). In the Mg^{2+} experiment, the half-maximal cleavage rate occured at a Mg^{2+} concentration which is higher than that in potassium chloride buffer (approximately 1 mM Mg^{2+}) (B.S.C. and A.W.N., unpublished experiments; see also [26]), and which may due to the chelating ability of glutamate [43]. Also, the true half-maximal concentration value in the Co^{2+} experiment may be somewhat lower than 3 mM, as Tris molecules are competitive Co^{2+} ligands [46]. (**B**) Autoradiogram of the Mn^{2+} experiment. Each lane contained 1000 dpm ^{32}P-labeled N26 RNA. The Mn^{2+} concentrations are: Lanes 1 and 2, 0.05 mM; lanes 3 and 4, 0.1 mM; lanes 5 and 6, 0.25 mM; lanes 7 and 8, 0.5 mM; lanes 9 and 10, 1 mM; lanes 11 and 12, 5 mM; lanes 13 and 14, 10 mM; lanes 15 and 16, 20 mM. Enzyme-independent cleavage of N26 RNA by Mg^{2+}, Mn^{2+} or Co^{2+} was not observed (data not shown). (**C**). Inhibition of RNase III processing by Zn^{2+}. The initial rate of ^{32}P-labeled N26 RNA cleavage (in reaction buffer containing 250 mM potassium glutamate and 5 mM Mg^{2+}, at 37°C) was measured as a function of added $CaCl_2$ or $ZnCl_2$. The data are plotted as percent maximal cleavage rate versus the Ca^{2+} (■) or Zn^{2+} (□) concentration.

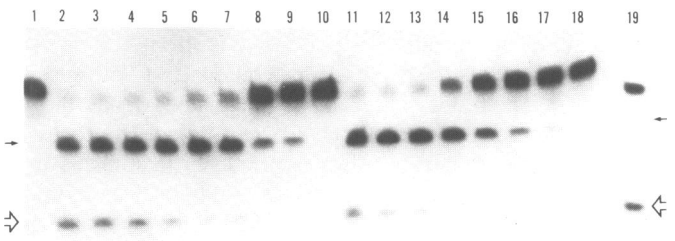

Figure 5. Glutamate anion effect on RNase III processing. Cleavage of ^{32}P-labeled N26 RNA (50 nM) by RNase III (10 nM) was carried out (2.5 min., 30°C) in reaction buffer containing 0−500 mM potassium glutamate or potassium chloride (addition of enzyme contributed 2 mM KCl to all reactions). Aliquots (2000 dpm) were analyzed by gel electrophoresis and autoradiography (see Materials and Methods). Lanes 1−9, potassium glutamate experiment. Lane 1 (no enzyme); lane 2, 0 mM; lane 3, 10 mM; lane 4, 40 mM; lane 5, 80 mM;, lane 6, 160 mM; lane 7, 250 mM; lane 8, 350 mM; and lane 9, 500 mM glutamate. Lane 10, 500 mM glutamate (no enzyme). Lanes 11−18, potassium chloride experiment, in the same order as in lanes 3−10. Lane 19, Mn^{2+}-dependent RNase III cleavage (run on a separate gel). In this experiment, the Mn^{2+} concentration was 5 mM, with no added monovalent salt. The small, closed arrow indicates the 38 nt product resulting from primary site cleavage, while the larger, open arrow indicates the 28 nt RNA produced by combined primary and secondary cleavage. Note in the Mn^{2+} experiment the relatively larger amount of the 28 nt (double cleavage) product, compared to the 38 nt (single cleavage) product. The 10 nt (5′ end-containing) and the 9 nt (3′ end-containing) product RNAs are not shown on this autoradiogram.

substrate complex, as shown by nondenaturing gel electrophoretic mobility shift experiments, and nitrocellulose filter binding assays (H.L., K.Zhang and A.W.N., unpublished results).

Monovalent salt and specific anion effects on RNase III processing

RNase III does not require a monovalent cation for activity, since R1.1 RNA can be efficiently processed in the absence of added salt (see Figure 5). Also, substitution of K^+ by NH_4^+ or Na^+ has no apparent qualitative or quantitative effect on R1.1 RNA cleavage (B.S.C. and A.W.N., unpublished experiments). However, the concentration of salt influences the pattern of processing. In low salt, the R1.1 RNA secondary site is efficiently cleaved in addition to the primary site (Figure 5, lanes 2−4, and 11−13). As the salt (potassium chloride or potassium glutamate) concentration increases, the primary site remains reactive, while secondary site cleavage is suppressed (Figure 5, lanes 5−9, and lanes 13−16). The low salt enhancement of secondary site processing may be formally related to the effect of Mn^{2+} or Co^{2+} substitution on RNase III activity (see Discussion).

Most *in vitro* studies of RNase III have employed reaction buffers containing chloride-based salts. However, it is not clear whether chloride represents an optimal anion for RNase III processing activity. Chloride is a minor species in the *E.coli* cytosol, which instead contains glutamate as the major anion, at a concentration of approximately 250 mM, with some variation [26,27]. Nucleic acid−protein interactions *in vitro* have been shown to be enhanced upon glutamate substitution [26,28]. To determine the effect of glutamate on RNase III processing, we assayed R1.1 RNA cleavage over a range of potassium glutamate or potassium chloride concentrations. To reveal any salt effects on either k_{cat} or K_m, the initial cleavage reaction was followed using a low concentration (relative to K_m) of substrate. The results of a representative experiment are shown in Figure 5. The

initial cleavage rate of R1.1 RNA diminishes at concentrations of potassium chloride above 80 mM, and is strongly suppressed by 500 mM. In contrast, potassium glutamate at 250 mM still allows efficient processing. Thus, glutamate extends the salt concentration range within which efficient RNase III processing can occur. The glutamate effect is primarily manifested in an enhanced turnover number (Table I). Additional experiments (data not shown) have shown that 250 mM glutamate also supports a greater percent conversion of precursor to product.

Can specific anions inhibit RNase III processing? For example, fluoride is an inhibitor of yeast inorganic pyrophosphatase [29]. We assayed the RNase III-catalyzed cleavage of ^{32}P-labeled R1.1 RNA, using reaction buffer containing potassium fluoride as the monovalent salt, at concentrations ranging up to 250 mM. The relative processing efficiencies were compared to those obtained using potassium glutamate-based reaction buffer. Fluoride at low concentrations (20 mM and below) does not inhibit the cleavage reaction. However, significant inhibition is seen at 100 mM fluoride, which is virtually complete by 250 mM (data not shown). Nondenaturing gel electrophoretic mobility shift and nitrocellulose filter assays (H.L. and A.W.N., unpublished experiments) reveal that fluoride does not block enzyme-substrate complex formation. A possible basis for the inhibitory effect of fluoride is discussed below.

DISCUSSION

This report describes new aspects of the physical and catalytic properties of RNase III, purified by an efficient procedure. RNase III processing *in vitro* obeys substrate saturation kinetics, indicating an overall reaction mechanism involving substrate binding at a specific site, followed by a chemical step and product release. The relative temperature-insensitivity of RNase III processing *in vitro* (at least in the 30−37°C range) may reflect the requirement for efficient RNA processing over the range of temperatures the cell may experience. Previous studies have noted the high catalytic efficiency of RNase III *in vivo*. In particular, the enzyme represents only 0.01% of cellular protein [15], yet effectively processes the large quantities of rRNA and mRNA precursors [30]. The measured *in vitro* catalytic efficiency of RNase III (3×10^7 l/mol-min) is comparable to that of *E.coli* RNase P (4×10^6 l/mol-min) [31] and *E.coli* RNase H (1.7×10^8 l/mol-min) [32], both of which are efficient *in vivo* activities. We therefore conclude that the *in vitro* processing activity of RNase III accurately reflects its *in vivo* catalytic efficiency, and that there is no need to invoke the existence of ancillary processing factors *in vivo* to confer full processing activity. In one instance, however, covalent modification (phosphorylation) can alter RNase III processing activity [33].

Glutamate anion extends the upper salt concentration range over which occurs the efficient *in vitro* processing of R1.1 RNA. Since the turnover number is preferentially enhanced under these conditions, glutamate apparently facilitates a step(s) occurring in the enzyme-substrate complex, including product release. In contrast, fluoride anion inhibits RNase III processing activity. Since gel electrophoretic mobility shift experiments indicate that fluoride does not block substrate binding, perhaps fluoride directly inhibits enzymic catalysis. In this regard, fluoride is a reasonably strong Mg^{2+} ligand [34], and may inhibit the binding and/or function of Mg^{2+} in the RNase III processing reaction.

RNase III cleavage of the R1.1 RNA secondary site increases as the monovalent salt concentration is lowered. The cleavage site corresponds to the secondary site within the T7 R0.3 [24] and R1.3 [8] processing signals. This cleavage behavior is consistent with earlier studies on the *in vitro* RNase III processing of the T7 polycistronic early mRNA precursor [20,24], wherein the monovalent cation concentration controls the reactivities of many secondary sites. Low salt may promote RNase III 'star' cleavage activity (see below), perhaps through enhanced binding of enzyme to suboptimal processing sites. However, assessing the influence of salt concentration on *in vitro* cleavage rates and reactivity patterns must take into account the reduced solubility of RNase III at low salt concentrations (see above).

RNase III processing of R1.1 RNA is supported by Mn^{2+} and Co^{2+}, in a manner similar to that exhibited by Mg^{2+}. It was originally reported that Co^{2+} is inhibitory [35]; however, the earlier study used impure enzyme. We find that Mn^{2+} at relatively low concentrations supports enzymatic cleavage of R1.1 RNA. This was also noted previously, using poly r(A-U) as substrate, with a main difference being that Mn^{2+} concentrations above 1 mM inhibited poly r(A-U) cleavage [21]. Again, the divergent results may have been due to impure enzyme employed in the original study. Neither Ca^{2+} nor Zn^{2+} support RNase III processing *in vitro*. Ca^{2+} has no effect on the Mg^{2+}-supported cleavage reaction, while Zn^{2+} can inhibit the reaction without blocking substrate binding. Perhaps Zn^{2+} occupies one or more Mg^{2+}-binding sites, thereby inhibiting the chemical step. Mn^{2+} and Co^{2+} stimulate cleavage of the R1.1 RNA secondary site. Mn^{2+}-activated RNase III secondary site cleavage (see also [24,25]) may be mechanistically similar to the effect of Mn^{2+} on other nucleic acid processing reactions, including restriction endonuclease-catalyzed cleavage of noncanonical sites [36,37]. In the latter case it has been proposed that the larger ionic radius of Mn^{2+}, and its greater ligand affinity constants promote recognition and cleavage of noncanonical recognition sequences, which may be suboptimally positioned within the enzyme active site [37]. It may therefore be useful to regard Mn^{2+}-activated RNase III processing as RNase III 'star' activity (also proposed elsewhere [7]), with the implicit assumption that the cleavage of secondary (suboptimal) sites reflects an intrinsically broadened processing capability of the Mn^{2+}-enzyme, rather than reflecting a Mn^{2+}-induced alteration of RNA structure. Whether the Mn^{2+}-RNase III complex is functionally important *in vivo* (e.g., see [25]) remains to be determined. A detailed description of the specific role of divalent cations in RNase III processing will require a variety of experimental approaches. However, the 5′ polarity of RNase III-catalyzed cleavage; the nonessential nature of the 2′-hydroxyl group adjacent to the scissile bond [12]; and the identification of a glutamic acid important for catalysis [7] formally raises the possibility of a 'two metal ion' mechanism for RNase III, as has been proposed for other phosphotransferases [38].

ACKNOWLEDGEMENTS

We thank June Snow of the Macromolecular Core Facility for synthesis of DNA oligonucleotides, and amino acid analyses. We also thank Drs F.W.Studier, J.J.Dunn and A.R.Rosenberg (Brookhaven National Laboratory) for supplying plasmids and *E.coli* strains, and Dr Michael Hagen (Center for Molecular Biology, Wayne State University) for instruction on the AMBIS radioanalytic imaging system. This study was supported by NIH Grant GM41283, and in part by the Center for Molecular Biology, Wayne State University.

REFERENCES

1. Gegenheimer P. and Apirion, D. (1981) Microbiol. Rev. *45*, 502–541.
2. Altman, S., Guerrier-Takada, C, Frankfort, H.M. and Robertson, H.D. (1982) in 'Nucleases' (S. M. Linn & R. J. Roberts, Eds.) Cold Spring Harbor Press, Cold Spring Harbor, New York, pp. 243–274.
3. King, T.C., Sirdeskmukh, R. and Schlessinger, D. (1986) Microbiol. Rev. *50*, 428–451.
4. Deutscher, M. (1988) Trends Biochem. Sci. *13*, 136–139.
5. Robertson, H.D. (1982) Cell *30*, 669–672.
6. Dunn, J.J. (1982) in 'The Enzymes' vol. 15 (P. Boyer, Ed.) Academic Press, NY pp. 485–499.
7. Court, D.L. (1992) in 'Control of mRNA Stability' (G. Brawerman and J. Belasco, Eds) Academic Press, New York (in press).
8. Saito, H. and Richardson, C.C. (1981) Cell *27*, 533–542.
9. Schmeissner, U., McKenney, K., Rosenberg, M. and Court, D. (1984) J. Mol. Biol. *176*, 39–53.
10. Regnier, P. and Grunberg-Manago, M. (1990) Biochimie *72*, 825–834.
11. Altuvia, S., Locker-Giladi, H., Koby, S., Ben-Nun, O., and Oppenheim, A.B. (1987) Proc. Nat. Acad. Sci. *84*, 6511–6515.
12. Nicholson, A.W. (1992) Biochim. Biophys. Acta *1129*, 318–322.
13. Nicholson, A.W., Niebling, K.R., McOsker, P.L. and Robertson, H.D. (1988) Nucleic Acids Res. *16*, 1577–1591.
14. Chelladurai, B.S., Li, H.L. and Nicholson, A.W. (1991) Nucleic Acids Res. *19*, 1759–1766.
15. Chen, S.M., Takiff, H.E., Barber, A.M., DuBois, W.C., Bardwell, J.C.A. and Court, D.L. (1990) J. Biol. Chem. *265*, 2888–2895.
16. March, P.E. and Gonzalez, M. (1990) Nucleic Acids Res. *18*, 3293–3298.
17. Robertson, H.D. (1971) Nature (New Biol.) *229*, 169–172.
18. Grodberg, J. and Dunn, J.J. (1988) J. Bact. *170*, 1245–1253.
19. Nashimoto, H. and Uchida, H. (1985) Mol. Gen. Genet. *201*, 25–29.
20. Dunn, J.J. (1976) J. Biol. Chem. *251*, 3807–3814.
21. Robertson, H.D., Webster R.E. and Zinder, N.D. (1968) J. Biol. Chem. *243*, 82- 91
22. Robertson, H.D. (1977) in 'Nucleic Acid-Protein Recognition' (H. Vogel, ed.) Academic Press, New York, pp. 549–568.
23. Dunn, J.J. and Studier, F.W. (1983) J. Mol. Biol. *166*, 477–535.
24. Gross, G. and Dunn, J.J. (1987) Nucleic Acids Res. *15*, 431–442.
25. Srivastava, R.K., Miczak, A. and Apirion, D. (1990) Biochimie *72*, 791–802.
26. Leirmo, S., Harrison, C., Cayley, D.S., Burgess, R.R. and Record, M.T. (1987) Biochemistry *26*, 2095–2101.
27. Richey, B., Cayley, D.S., Mossing, M.C., Kolka, C., Anderson, C.F., Farrar, T.C. and Record, M.T. (1987) J. Biol. Chem. *262*, 7157–7164.
28. Zou, L. and Richardson, J.P. (1991) J. Biol. Chem. *266*, 10201–10209.
29. Baykov, A.A., Bakuleva, N.P., Nazarova, T.I., and Avaeva, S.M. (1977) Biochim. Biophys. Acta *481*, 184–194.
30. Dunn, J.J. and Studier, F.W. (1973) Proc. Nat. Acad. Sci. *70*,3296–3300.
31. Guerrier-Takada, C., Gardiner, K., Marsh, T., Pace, N.R. and Altman, S. (1983) Cell *35*, 849–857.
32. Kanaya, S., Kohara, A., Miura, Y., Sekiguchi, A., Iwai, S., Inoue, H., Ohtsuka, E. and Ikehara, M. (1990) J. Biol. Chem. *265*, 4615–4621.
33. Mayer, J. E. and Schweiger, M. (1983) J. Biol. Chem. *258*, 5340–5343.
34. Sienko, M. and Plane, R.A. (1974) 'Chemical Principals and Properties' McGraw-Hill, New York.
35. Paddock, G.V., Fukada, K., Abelson, J. and Robertson, H.D. (1976) Nucleic Acids Res. *3*, 1351–1371.
36. Hsu, M.T. and Berg, P. (1978) Biochemistry *17*, 131–138.
37. Selent, U., Ruter, T., Kohler, E., Liedtke, M., Thielking, Alves, J., Oelgeschlager, T., Wolfes, H., Peters, F. and Pingoud, A. (1992) Biochemistry *31*, 4808–4815.
38. Beese, L.S. and and Steitz, T.A. (1991) EMBO J. *10*, 25–33.
39. Studier, F.W. (1973) J. Mol. Biol. *79*, 237–248.
40. Oakley, J.L. and Coleman, J.E. (1977) Proc. Nat. Acad. Sci. USA *74*, 4266–270.
41. Milligan, J.F., Groebe, D.F., Witherell, G.W. and Uhlenbeck, O.C. (1987) Nucleic Acids Res. *15*, 8783–8798.
42. Szewczak, A.A., White, S.A., Gewirth, D.T. and Moore, P.B. (1990) Nucleic Acids Res. *18*, 4139–4142.
43. Han, H., Rifkind, J.M. and Mildvan, A.S. (1991) Biochemistry *30*, 11104–11108.